



A Single-Cell Translocation and Secretion Assay (TransSeA)

Journal:	<i>Lab on a Chip</i>
Manuscript ID	LC-ART-08-2018-000821
Article Type:	Paper
Date Submitted by the Author:	08-Aug-2018
Complete List of Authors:	<p>Cai, Wei; University of California San Diego, Materials Science and Engineering Chiu, Yu-Jui; University of California San Diego, Materials Science and Engineering Ramakrishnan, Valya; University of Minnesota System, Department of Neurosurgery Tsai, Yihuan; University of California San Diego, Materials Science and Engineering Chen, Clark; University of Minnesota System, Department of Neurosurgery Lo, Yu-Hwa; University of California, Department of Electrical and Computer Engineering; University of California San Diego, Materials Science and Engineering</p>

A Single-Cell Translocation and Secretion Assay (TransSeA)

Wei Cai^{1,#}, Yu-Jui Chiu^{1,#}, Valya Ramakrishnan², Yihuan Tsai¹, Clark Chen^{2,*}, and Yu-Hwa Lo^{1,3,*}

¹Materials Science and Engineering Program, University of California at San Diego, La Jolla, California, USA; ²Department of Neurosurgery, University of Minnesota, Minneapolis, Minnesota, USA; ³Department of Electrical and Computer Engineering University of California at San Diego, La Jolla, California, USA

*These authors are joint senior authors on this work

#These authors contributed equally to this work

For correspondence: Clark C. Chen (ccchen@umn.edu) and Yu-Hwa Lo (ylo@ucsd.edu)

Understanding the biologic heterogeneity at the single cell level is required for advancing insights into the complexity of human physiology and diseases. While advances in technologic and analytic methods have afforded unprecedented glimpses of this heterogeneity, the information captured to date largely represents one-time “snap” shots of single cell physiology. To address the limits of existing methods and to accelerate discoveries from single cell studies, we developed a single-cell translocation and secretion assay (TransSeA) that supports time lapse analysis, enables molecular cargo analysis of secretions such as extracellular vesicles (EVs) from single cells, allows massively parallel single cell transfer according to user-defined cell selection criteria, and supports tracking of phenotypes between parental and progeny cells derived from single cells. To demonstrate the unique capabilities and efficiencies of the assay, we present unprecedented single cell studies related to cell secretions, EV cargos and cell intrinsic properties. Although used as examples to demonstrate feasibility and versatility of the technology, the studies already produce insights on key unanswered questions such as the micro RNAs carried by EVs, the relations between EV secretion rate and gene expressions, and the spontaneous, trans-generational phenotypic changes in EV secretion between parental and progeny cells.

Introduction

There is increasing appreciation that understanding the compositional heterogeneity at the single cell level is required for advancing insights into the complexity of human physiology and diseases (¹⁻⁴). While advances in technologic and analytic methods have afforded unprecedented glimpses of this heterogeneity (⁵⁻⁹), the information captured to date largely represented single-time “snap” shots of single cell physiology (¹⁰⁻¹⁵). Whether this physiology remains static or dynamically evolves as a function of cell passage remains a fundamental and unanswered question, mainly because of lacking effective tools to conduct such studies. Missing such vital information can cause loss of major insights and opportunities for understanding and discovering methods of treating diseases as biological systems are inherently heterogeneous and dynamic.

Another deficiency of the current single-cell assay based on single-cell RNA sequencing and phenotyping is the lack of information for secretions from each single cell. This, again, can lose vital insight given that cell secretions are the means for cell-cell communications and related closely to cancer growth and metastasis. Among the key components of cell secretions are extracellular vesicles (EVs) such as exosomes. EVs are nano-sized, membrane bound vesicles that are released by all cell types (¹⁶). They have been shown to contain proteins as well as a range of nucleic acids, including DNA, mRNAs, and miRNAs, which can be transferred to target cells, thereby modulating the activities of these recipient cells (¹⁷) as well as mediating cell-to-cell communications (¹⁸⁻²⁰). Most studies in the biogenesis of extracellular vesicles are performed over a cell population, in which the unique behaviors of minority or individual cells are masked (²¹⁻²⁷).

To address the above deficiencies in today’s single-cell analysis, we present an open platform (i.e. open to media change and modifications of microenvironments) single-cell Translocation Secretion Assay (TransSeA) for parallel single cell analysis with the following salient features: (a) locating and tracking single cell behaviors as well as single cell secretions to enable correlation studies between phenotypes and secretion patterns or cargos of EVs, (b) enabling massively parallel translocation of single cells by user defined criteria, and (c) allowing continual growth and development of single-cell derived micro colonies to support studies of single-cell genealogy and hereditary properties. The combination of the above three capabilities plus the open platform facilitating media change and modifications of microenvironments offer enormous flexibilities and capabilities for single cell studies in high efficiency. Using this platform, we demonstrate transgenerational phenotypic changes in extracellular vesicle (EV) secretion between parental and progeny cells.

Results and Discussions

TransSeA Technology

The open platform of the single-cell translocation and secretion assay (TransSeA) has three technology components: templates for single cell culture^{28,29}, single cell secretion harvesting, and parallel translocation of targeted cells. The assay provides an enabling tool to link individual cell behaviors, especially behaviors of rare cells, and single-cell genomics in a highly efficient manner. The overall work flow of the TransSeA is shown in Fig 1. The first part of TransSeA is a single cell culture chip (Fig. 1A) consisting of a polyester thin film filter attached to a layer of PDMS through-holes²⁸. The polyester filter provides substrate for cell attachment and the PDMS through-holes provide physical confinements and position registrations of individual cells. The pore size of polyester thin film filter (e.g. 0.8 μ m) is chosen to allow passing of cell secretions while supporting the cells. The single cell culture chip is assembled into a CNC (Computer Numerical Control) machined fixture. The assay offers two alternatives, one being target specific and another being holistic (Fig. 1B), to noninvasively collect and capture secretions from each single cell at registered positions. For target specific capturing, one can periodically place a glass plate coated with specific probes such as anti-CD63 antibody for capture of CD63 positive EVs (³⁰⁻³²) atop the cell culture fixture with a spacing of 100 μ m. After fixation of the CD63+ EVs on the glass plate, the CD63+ EVs secreted by all single cells can be preserved for months to show the history of the secretion pattern of each single cell and reveal cell behavior changes over its life cycle and under influences of drugs or toxins. The information is highly quantitative as one can enumerate EVs secreted at each time point by labelling the captured EVs with another anti-CD63 that is biotinylated to bond with a streptavidin-conjugated quantum dot. Alternatively, if applications require collection of all secretions in suspension for downstream process rather than specific secretions immobilized on a glass substrate, secretions can be drained into microwells underneath the cell culture fixture via the pores of the filter. In this paper, we study EVs secretion rate as an example for quantitative single cell analysis with TransSeA while the assay works for cytokines as well.

Another key feature of single-cell TransSeA is to allow users to select individual cells of particular interest according to their phenotype, antibody labeling, FISH labeling, secretion properties^{1,2,33}, etc. and isolate and transfer them in a massively parallel manner to a new template while keeping track of the position and identity of cells. To demonstrate such unique capabilities, we selected specific single-cell derived micro colonies for further studies following the steps illustrated in Fig. 1(C).

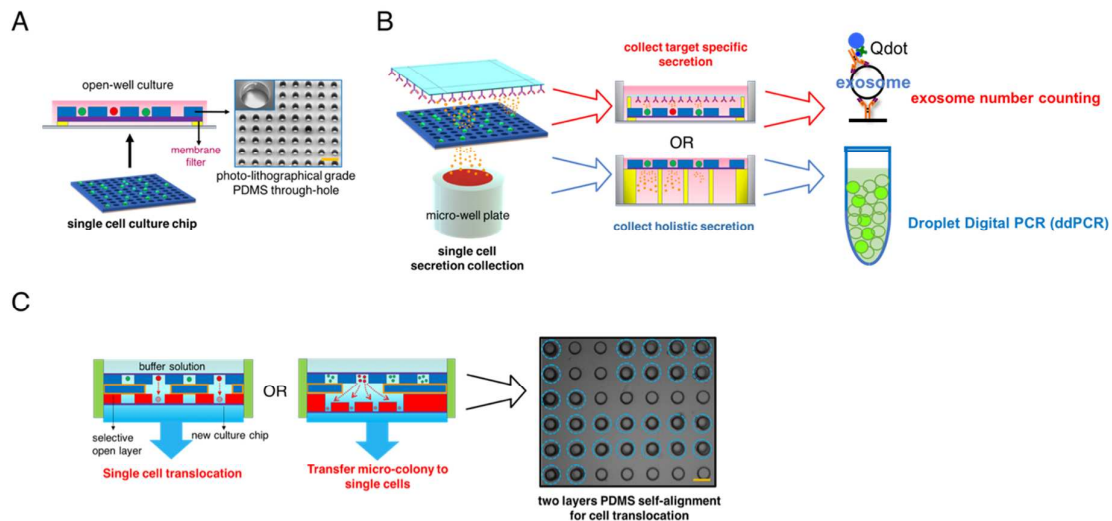


Figure 1 Single cell culture, single cell secretion harvesting, EVs collection for downstream process and parallel cell transfer of TransSeA. (A) Single cell culture chip consisting of a polyester thin film filter attached to a layer of PDMS through-holes for single cell positioning and culture. The scale bar represents 0.1 mm (B) Two methods for collecting single cell secretions: target specific collection by an antibody functionalized plate atop the device and holistic collection of single cell secretions by microwells beneath the device. Collection of holistic EVs secretion for Droplet Digital PCR (ddPCR). (C) Parallel cell transfer. The positions of user-selected cells on the cell culture chip, marked red, are mapped onto a UV-patterned PDMS through-holes. Guided by the UV-PDMS pattern, each targeted cell in each well is translocated to a new single-cell culture chip (e.g. 80 μm diameter through-holes attached to a 0.8 μm pore polyester filter). The blue circles are the positions of user-selected opening on UV-patterned PDMS device. The scale bar represents 0.1 mm.

Target cell selection and massively parallel cell transfer of TransSeA

One bottleneck in massive single cell analysis is cell isolation on demand in a precise and parallel manner. Cell selection and isolation by fluorescent activated cell sorter (FACS) loses track of the history of the cell behaviors. On the other hand, any single cell aspiration

process such as automated pico-pipettes suffers from low throughput and high risk of cell stress by handling with mechanical forces (^{34–36}). The TransSeA assay addresses this problem with a user-defined parallel cell translocation approach elucidated next.

After users decide which single cells over the cell plate are worth further studies based on such criteria as phenotypes, biomarkers, secretions, etc., a 2-D pattern of PDMS through-holes is formed corresponding to the positions of selected cells (Fig. 2A). The user-defined pattern can be generated in an automated fashion with a software relating the user-defined criteria to the cell registration pattern from a microscope image. This cell transfer pattern is used to create PDMS through holes to guide the cell transfer process, while keeping those non-selected cells in place for other studies and allowing cell transfers for multiple times under different selection criteria. Different from conventional PDMS soft lithography process that requires lithographic masks and cleanroom fabrication of the mold, the user-defined PDMS through-holes used to guide the cell transfer are produced directly with UV-patternable PDMS that requires no solvents or a cleanroom facility (details in **Materials and Methods**). Therefore, the process can be performed rapidly in typical biomedical or clinical laboratories to realize user-defined parallel single-cell transfer. Fig. 2B demonstrates such massively parallel cell transfer capabilities. Another single-cell culture chip, consisting of a prefabricated 2D through-holes (80 μm diameter) attached to a polyester filter, is placed on the opposite side of the original cell culture chip to receive the transferred cells. Between the original cell culture chip and the cell receiving chip is the user-defined PDMS through-holes that define the locations of cells to be transferred. A microfluidic flow that drives the chosen cells from their original template to the receiving template is produced by applying a vacuum (~ 0.7 atm) from the cell receiving end to suck the liquid (1X PBS) atop the cell transmitting end. For adherent cell lines, a standard trypsin contained buffer can substitute PBS buffer to dissociate cells before cell transfer. To easily visualize cell transfer over a large area, we have used GFP-labelled glioblastoma (a highly malignant form of brain cancer (¹⁷)) CMK3 cells (Department of Neurosurgery, University of Minnesota, Minneapolis) with high cell concentrations to populate each position with multiple cells. A detailed characterization of the process shows that the cell transfer process produces high position precision ($<1\%$ misplaced cells) and transfer yield with $<10\%$ cell loss (Fig. 2D).

Beyond the cell transfer process described above, in the following we demonstrate the versatility of the assay by showing the method of transferring single-cell derived

microcolonies into a receiving single-cell culture chip (Fig. 2C). The method uniquely enables studies of heredity and dynamics of cells in proliferation.

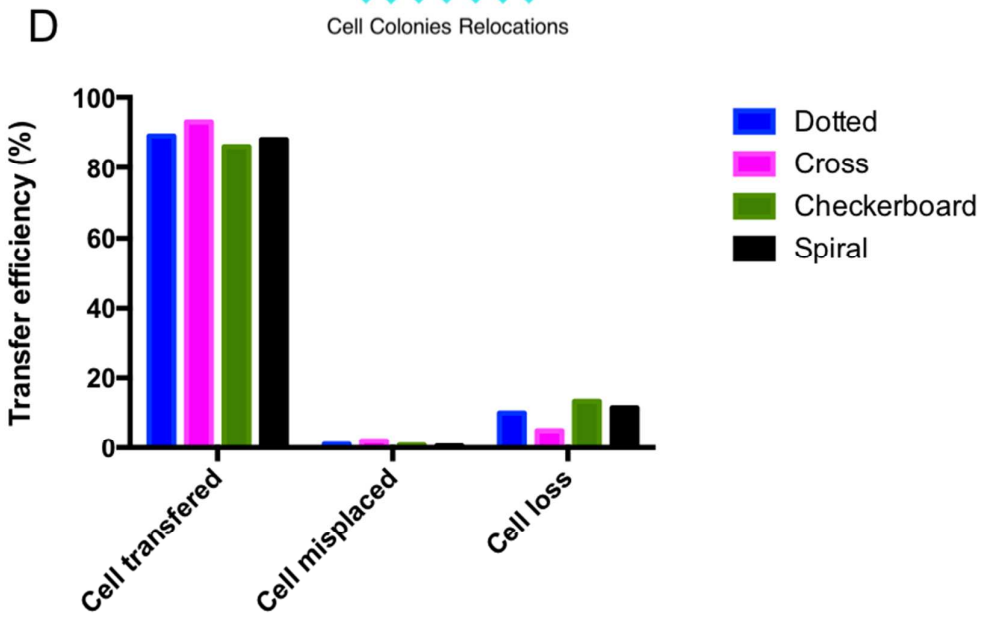
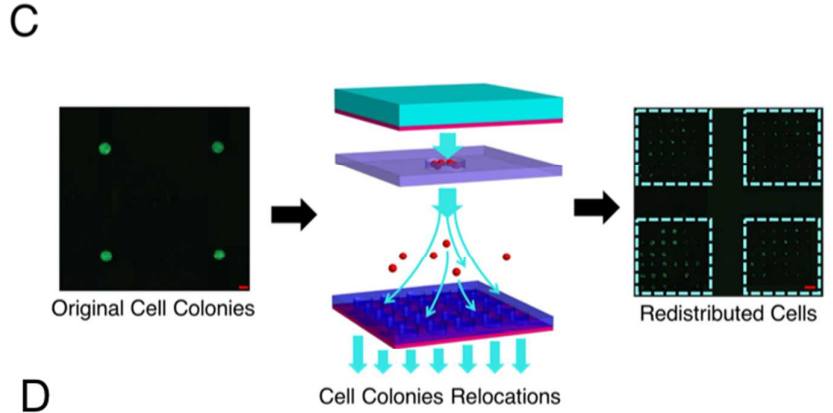
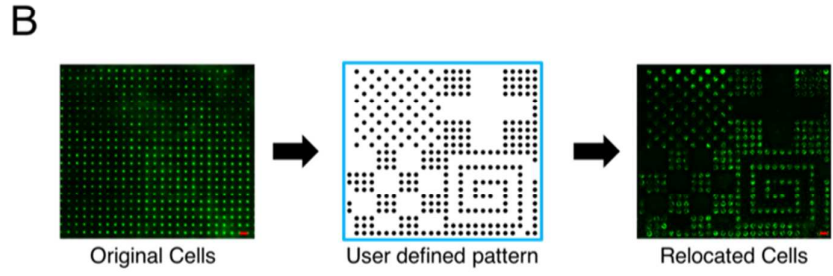
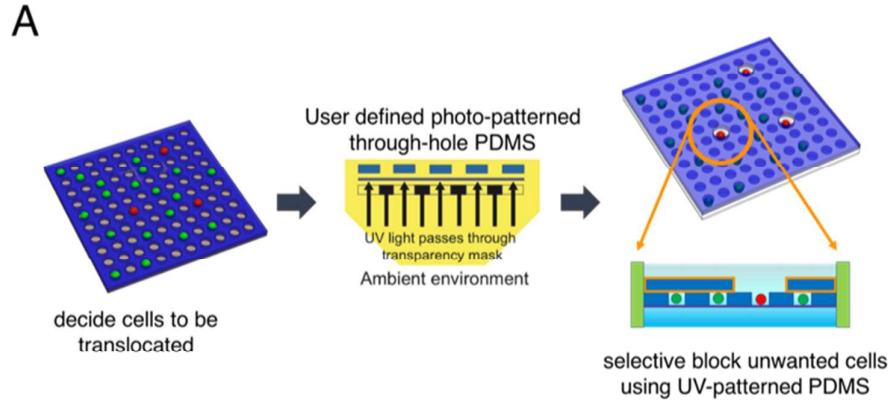


Figure 2 Parallel cells transfer. (A) Process flow for massively parallel single cell transfer according to a user-defined pattern. (B) Demonstration of cell transfer. A UV-sensitive PDMS through-holes with user-defined patterns (middle layer) was used to transfer GFP-transfected CMK3 cells to a plate. Different patterns are used to show the transfer efficiency. Pattern 1: Dotted; Pattern 2: Cross; Pattern 3: Checkerboard; Pattern 4: Spiral. To easily visualize cell transfer over a large area, we have used GFP-labelled cells with high cell concentration. (C) A varied version of TransSeA to distribute single-cell derived microcolonies onto a single cell chip for the progeny cells. The left panel shows 4 single-cell derived microcolonies and the right panel shows how the progeny cells of each microcolony is redistributed onto an array of single cells. The scale bar represents 0.4 mm. (D) Cell transfer efficiency.

Inhomogeneity in single cell EV secretion rate

Analysis of 193 GFP-labelled glioblastoma CMK3 single cells revealed EV secretion rate varying over two orders of magnitude, ranging from 2 to 218 CD63+ EV per 3 hours collection period. Whereas our previous studies demonstrate that these single cells are genetically isogenic within inherent statistical error of exome sequencing (³⁷), it is surprising to find that such genetically isogenic cells display large diversity in their EV secretion rate. The distribution for EV secretion rate cannot be fitted by a single Gaussian or other typical distribution function used to model biological systems because of its significantly greater populations in the long tail several standard deviations away from the mean value. Instead, the distribution was best fitted by two distinct Gaussian distributions, with a “low EV-secreting” population (mean secretion rate of ~ 40 CD63+ EV per 3 hour) and a “high EV-secreting” population (mean secretion of ~ 115 CD63+ EV per 3 hours; **Fig 3**). This property seems to suggest that genetically identical glioblastoma single cells exhibit distinct cell states with different EV secretion rates.

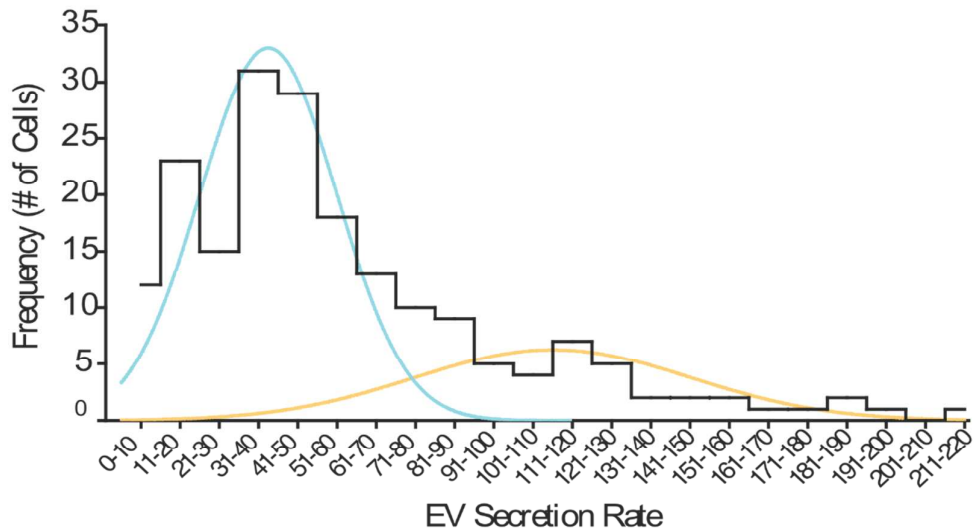


Figure 3 Summary of EVs secretion rate from 193 single cells. The data show extraordinarily large inhomogeneity in EVs secretion rate among individual cells and cannot be fitted by a single Gaussian or other typical distribution function. They are best fitted by two distribution curves, one with an average secretion rate of around 40 EVs per 3 hours and another with an average secretion rate of 115 EVs per 3 hours.

Exosomal miRNA from single cells

Exosomal miRNAs represent a particularly attractive biomarker platform for ‘liquid biopsies’. miR-21 is a miRNA that is highly over-expressed in glioblastoma cells³⁸. The expression of miR-21 in glioblastoma mediates several essential oncogenic functions, including suppression of apoptosis, growth proliferation and tolerance of DNA damages. We therefore use TransSeA to test the secretion rate and exosomal miR-21 expressed by single cells. We use droplet digital PCR (ddPCR) to test the copy number of miR21 carried by exosomes secreted by each glioblastoma cell. Since our main purpose here is to demonstrate the feasibility of testing the EV secretion rate and miR carried by the EVs as molecular cargo, we randomly choose only 5 cells and the test results are shown in Figure 4. Interestingly, this preliminary result reveals positive correlations between the EV secretion rate and the miR-21 copy numbers carried by the EVs.

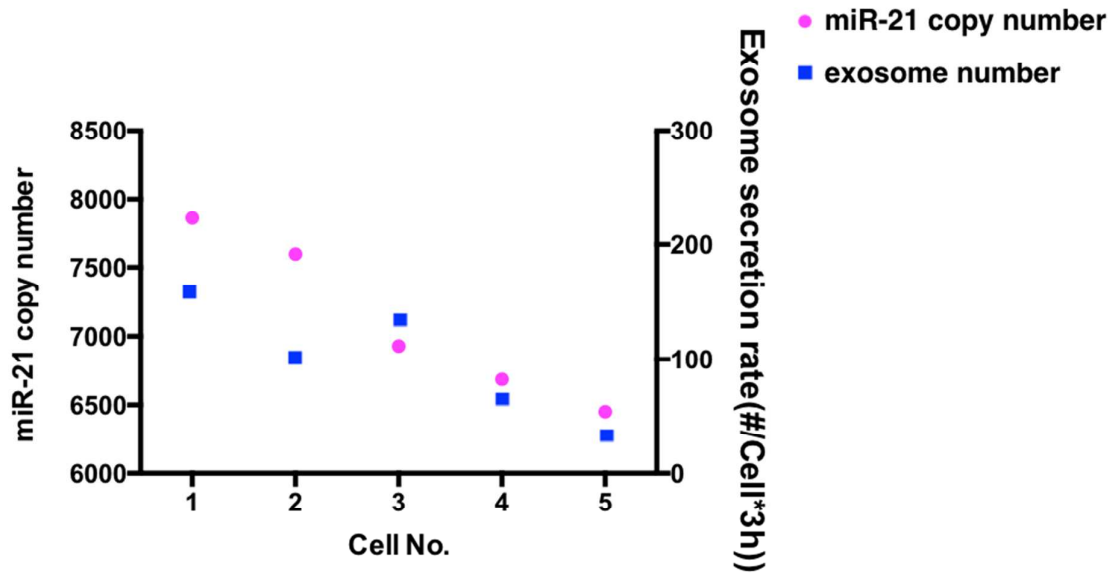


Figure 4 Total exosomal miR-21 copy number in culture media measured by ddPCR and exosome secretion rate from five single cells, as demonstration of the versatility of TransSeA.

EVs secretion rate hereditary through cell genealogy

One unanswered question that could have significant ramifications in fundamental and clinical biomedicine is whether and to what extent EV secretion of a cell is hereditary. In other words, whether EV secretion rate is an intrinsically static, hereditary property or one undergoing dynamic, spontaneous changes.

After quantification of CD63+ EV secretion rate, the CMK3 single cells were classified as low or high secretors (**Fig 3**) and cultured for an additional 72 hours to generate micro-colonies of 2 to 6 cells representing 1-3 generations of cell division. These micro-colonies were transferred to a second single cell culturing chip using the aforementioned design such that each of the progeny cells was cultured individually (**Fig 5A**). Using the process described previously, those chosen single-cell derived microcolonies were translocated from the original cell plate to a new cell plate via the user-defined PDMS through holes. Furthermore, the cells belonging to the same microcolony were channeled by another pre-defined 80 μm through-holes to become individual cells residing on the filter template (**Fig 5A**). CD63+ EV secretion rate was then determined for each progeny cell and compared to the parental rate. **Fig 5 (B)** shows an analysis of 14 lineages derived from 10 low and 4 high CD63+ EV secretors. ~20% of the progenies of low CD63+ EV secretors became high EV secretors and most surprisingly, ~75% of the progenies of high CD63+ EV

secretors became low EV secretors. The study suggests that the EV secretion rate does not show an obvious hereditary trait and low EV rate appears to be normal for CMK3 cells (since most High EV cells produced low EV descents) while some low EV cells can occasionally (around 20% chance) produce high EV descents. Although further studies are needed to conclude if the findings are specific to the chosen cell type or a more general phenomenon for different types of cells, the study demonstrates the unique capability of the TransSeA as an enabling technique to investigate key unanswered questions in biomedicine.

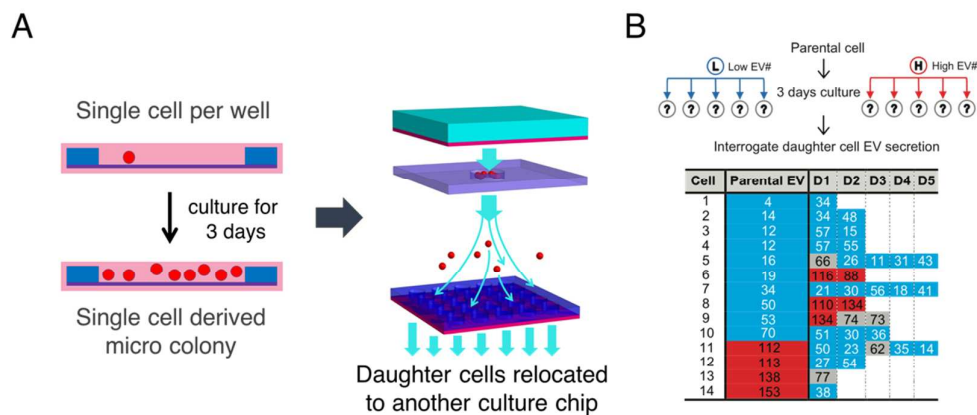


Figure 5. Parallel cell transfer and study of EVs secretion rate heredity through cell genealogy. (A) A single cell derived micro-colony was transferred to a new single cell culture chip to allow monitoring the EV secretion rate of each individual progeny cell. (B) The EVs secretion rates of those progeny cells from 14 parental cells. Cells secreting less than 60 EVs in 3 hours were labelled as Low EV (blue) and cells secreting more than 80 EVs in 3 hours were labelled as High EV (red). Those cells that secreted 61 to 80 EVs in 3 hours were considered to have an intermediate secretion rate (grey). D1 to D5 refer to daughter cells 1 to 5

Dependence of gene expressions and EV secretion rate for single cells

We next use TransSeA to test whether EV secretion rate is a function of the intrinsic physiology of the single cell. While the mechanism underlying EV secretion remains poorly understood (^{38,39}), increased EV secretion has been associated with neoplastic transformation (⁴⁰⁻⁴²). We therefore tested whether EV secretion is correlated with the expression of key genes implicated in glioblastoma pathogenesis, including MYC (^{37,43}) and OLIG2 (^{43,44}). EV

secretion rate of single cells was determined and categorized as low (<60) and high (>80) secretors. Random clones of low and high secreting single cells were then subjected to qPCR for MYC and OLIG2 expression. We observed an positive correlation between EV secretion rate with MYC ($p=0.0098$, **Fig 6A**) and OLIG2 ($p=0.0127$, **Fig 6B**). Importantly, combination of MYC and OLIG2 better segregate with the EV secretion rate than each individually (**Fig 3C**). These results suggest that EV secretion in glioblastoma is dictated by the physiologies mediated by MYC and OLIG2.

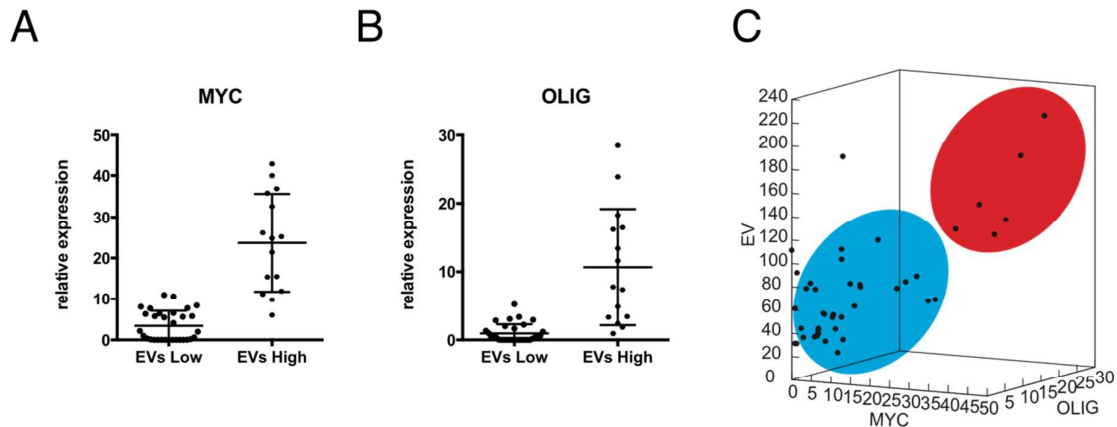


Figure 6 Relation between EV secretion rate and gene expression. (A) Correlation of MYC expression to EV secretion ($p=0.0098$). (B) Correlation of OLIG expression to EV secretion ($p=0.0127$). (C) EV secretion rate and expressions of MYC and OLIG shows two distinct distributions of CMK3. The p-value was fitted by a linear line.

Conclusion

To summarize, we present a single-cell Translocation Secretion Assay (TransSeA) that offers a myriad of unique capabilities for investigations of single cells, including quantifying single cell secretions and molecular cargos such as mi-RNAs carried by exosomes, and relating single cell secretions and their intrinsic properties such as gene expressions. The open platform of TransSeA allows easy access and control of microenvironments, supports cell tracking, time lapse analysis, as well as parallel translocation of single cells and single-cell derived micro colonies based on user-defined criteria and biomarkers. The TransSeA fills the gap between standard FACS-based cell sorting and massive sequencing in the single-cell work flow. By way of examples, we use TransSeA to study the relations between cell EVs secretion rate and its genealogy and gene expressions, with the purpose of demonstrating the unique capabilities of TransSeA for quantitative analysis of single cell

biology. TransSeA should enable future investigations that yield insights into the dynamic nature of cell states in single cells, with implications to physiologic and pathologic processes.

Materials and Methods

Chip fabrication process for single cell placement and culture

The single cell culture chip is made of a layer of PDMS through-holes bonded to a PETE membrane filter. Its fabrication process flow is summarized in Fig. 7. First we describe the fabrication process for PDMS through holes using a lift-off (peel-off) process²⁸. A layer of 6 μm thick NR9-3000PY negative photoresist (Futurrex, Frankling, NJ, USA) was used to define the through-hole pattern. Having the photoresist layer as etch mask, a 2D array of 50 μm deep, 40 μm diameter mesas were formed by deep reactive ion etching (DRIE) process (Oxford Plasmalab 100) (Fig. 7 C). The etched Si wafer was spin-coated (1500 rpm for 60 seconds) with ~ 50 μm thick uncured PDMS (Sylgard 184, Dow Corning, MI) premixed with hexane in 1:1 ratio (v/v) (Fig. 7D). The PDMS-coated wafer was baked in a 65°C oven for 90 minutes. To provide mechanical strength for easy handling, a 2 mm thick PDMS ring surrounding the 2D array pattern area was attached to the Si wafer. After curing the PDMS ring in a 65°C oven for 90 minutes, the entire wafer was immersed in acetone and sonicated for 5 minutes twice to lift off the PDMS layer on top of the 50 μm high etched Si mesas. PDMS lift-off was obtained because the amount of photoresist swelling in acetone broke the sidewall coating of PDMS. After the PDMS lift-off process, the wafer was rinsed with methanol and isopropanol and dried with nitrogen gas (Fig. 7 E). After baking the wafer in a 75°C oven for 5 minutes to evaporate any solvents trapped in the PDMS layer on the bottom of the Si mesas, one could easily separate the PDMS from the Si wafer by holding the PDMS ring to obtain a 2D array of PDMS through holes that are 40 μm in diameter and 50 μm deep in this case. Using the same process by varying the parameters, one can fabricate PDMS through-holes of different dimensions and geometries.

To choose a surface to hold the cells, we used polyester (PETE) membrane filters with 0.8 μm pores which allow cell seeding and at the same time, collection of cell secretions through the membrane pores into the microwells underneath. To bond the PDMS film with through-holes onto the PETE membrane filter, the PETE membrane was activated in an oxygen plasma chamber for 7 mins (600 mTorr, 100 W) and then immersed for 5 minutes in a 5% water diluted APTES (Sigma-Aldrich, St Louis, USA) solution on a 80 °C hot plate. The APTES solution was covered during the heating process to prevent water evaporation. Afterwards the APTES treated PETE membrane was bonded to the oxygen plasma activated (600 mTorr, 100 W) PDMS film with through-holes (Fig. 7 F). When the PETE membrane was brought to contact with the PDMS through-hole film, an irreversible bond was formed

almost immediately (Fig. 7 G). After the bonded sample was dried in air for 24 hours, the chip was ready for single cell placement and culturing.

To load cells onto the chip, the cell suspended medium was dispensed on the chip surface and went through centrifuge for 1 minute. The eccentric force drove the cells onto the PETE membrane filter via the PDMS holes as guide channels. Any extra cells outside the PDMS holes were flush away with buffer solution.

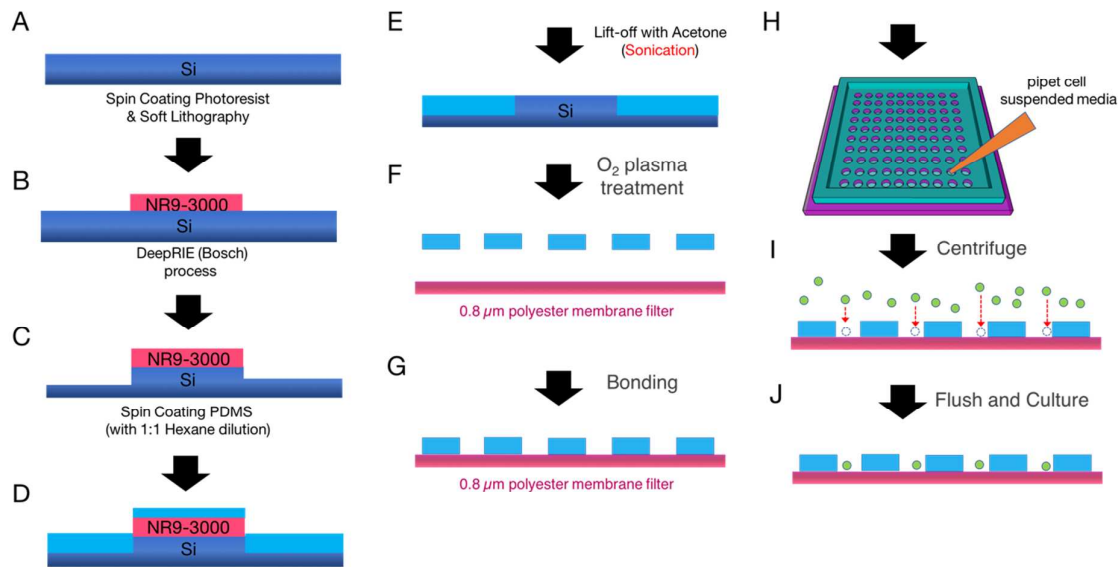


Figure 7. Chip fabrication (A-G) and single cell loading process (H-J). (A) Prepare a clean Si-wafer (B) Form 6 μm thick photoresist NR9-3000 PY patterns. (C) Using photoresist as mask for Deep RIE Si etch to form 50 μm deep, 40 μm diameter mesas. (D) Spin coat PDMS with 1:1 hexane dilution (E) lift-off the PDMS atop the photoresist with acetone. (F) PDMS through-holes (meshes) are formed after separating the PDMS film from the Si mold. Both the PDMS surface and a polyester (PETE) membrane filter are treated with oxygen plasma. (G) The PDMS film with through-holes are bonded to the polyester membrane filter to form the single cell culture chip. (H)-(J) Cells are loaded to a single cell culture chip by centrifuge. Around 70% positions contain single cells in an optimized process²⁷.

Fabrication of user-defined PDMS through-holes to guide transfer of selected cells

The UV-patternable PDMS (UV-PDMS) fabrication process is shown in Fig. 8. The positions of user-selected cells are first printed on a transparency mask using an office-grade laser printer. UV curable PDMS is coated on a piece of cover glass. A UV lamp (100 W, about 0.5 W/cm²) is used to illuminate the UV curable PDMS through the transparency mask

for 20 seconds. After washing off the uncured UV-PDMS by sonication in the water bath for 15mins, the patterned UV-PDMS film is peeled off from the cover glass. The entire process uses only water without aggressive or toxic chemicals and requires no sophisticated cleanroom microfabrication equipment. Hence it can be done in a standard biological laboratory by researchers following a straightforward protocol.

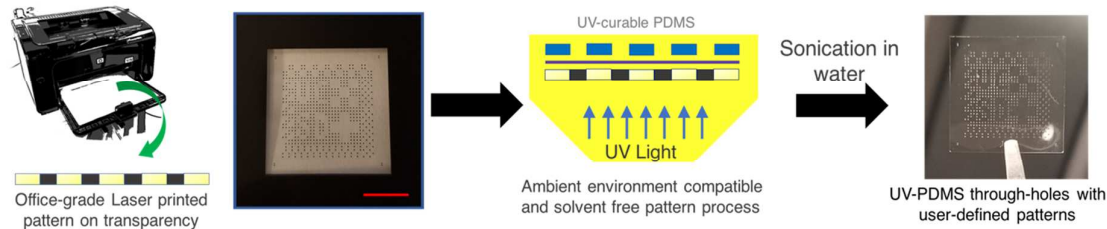


Figure 8. Fabrication of user-defined PDMS through-holes to guide transfer of selected cells. At first, print the positions of user-selected cells onto a transparency mask using an office-grade laser printer. Coat UV-patternable PDMS (UV-PDMS) on a piece of cover glass and placed it on top of the transparency mask. Expose the UV-PDMS through the mask by a UV lamp (100 W, about 0.5 W/cm^2) for 20 seconds. The UV-cured PDMS is removed from the cover glass by sonication in a water bath. The scale bar is 5 mm.

Cell Transfer Assembly

Figure 9 shows schematically the design of cell transfer device. A machined fixture is fabricated to house the cell transfer chip assembly. The chip assembly, from top to bottom, comprises a cell culture chip containing the single cells to be selectively transferred (top/red), a layer of user-defined UV-PDMS patterned through-holes (middle/yellow), and another cell culture chip to receive the transferred cells (bottom/blue). The cell transfer assembly is fitted into a 3D printed water sealed chamber. By applying a vacuum ($\sim 0.7 \text{ atm}$) from the cell receiving end to suck the liquid (1X PBS) atop the cell transmitting end, the microfluidic flow drives the chosen cells from their original template to the receiving template.

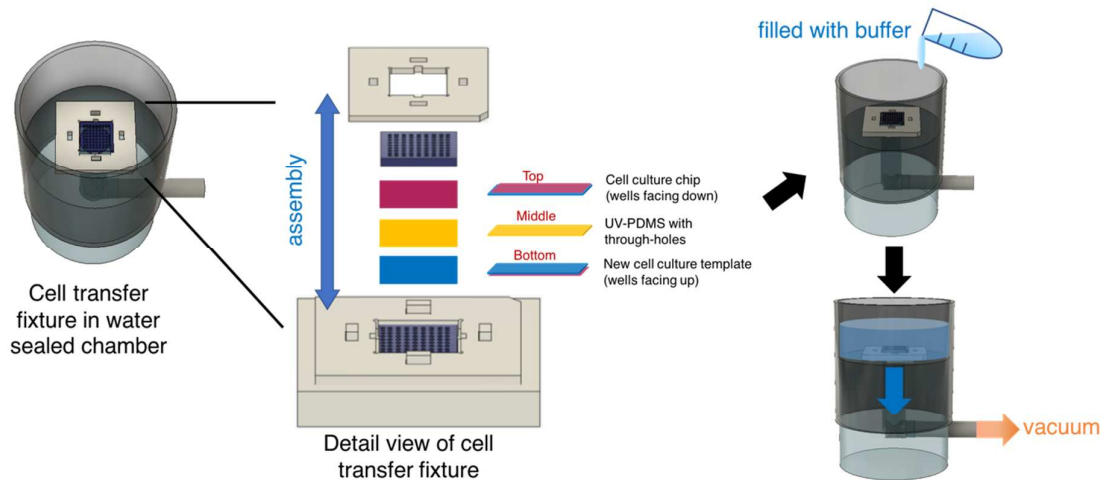


Figure 9. Schematics of cell transfer assembly. A cell transfer fixture shown at center is assembled with the sandwiched structure of cell culture chip (top/red), user-defined UV-PDMS through-holes (middle/yellow), and new cell culture template (bottom/blue). The sandwiched structure is placed in a 3D printed water sealed chamber. The assembly is then filled with buffer solution and vacuumed to accomplish the cell transfer.

Droplet Digital PCR

All the EVs from single cells were lysed in 9ul lysis buffer (50mM Tris HCl pH 8, 140mM NaCl, 1.5mM MgCl₂, 250μl IGEPAL) containing 1mg/ml BSA³⁷. Immediately before EV lysing, 5ul/ml RNasin Ribonuclease Inhibitor (Promega, Madison, WI) was added to protect miRNA from RNases in the following cDNA synthesis reactions. Cells were lysed by gentle rocking at room temperature for 10 minutes. The lysed cells were maintained on ice before cDNA synthesis. cDNA synthesis was performed using TaqMan™ MicroRNA Reverse Transcription Kit (ThermoFisher Scientific, Santa Clara, CA) per manufacturer's instructions. cDNA was preamplified using Taqman Preamp Master mix (ThermoFisher Scientific, Santa Clara, CA) per manufacturer's instructions. Droplet Digital PCR was performed to assess the expression of miR-21 using QX200™ Droplet Digital™ PCR System (Bio-Rad).

Single Cell qPCR

Each single cell was lysed in 11ul lysis buffer (50mM Tris HCl pH 8, 140mM NaCl, 1.5mM MgCl₂, 250μl IGEPAL) containing 1mg/ml BSA³⁷. Immediately before cell lysing, RNasin Ribonuclease Inhibitor (Promega, Madison, WI) was added to protect mRNA from RNases in the following cDNA synthesis reactions. Cells were lysed by gentle rocking at room temperature for 10 minutes. The lysed cells were maintained on ice before cDNA

synthesis. cDNA synthesis was performed using iScript Advanced cDNA synthesis kit (Bio-Rad, Hercules, CA) per manufacturer's instructions. cDNA was preamplified using Taqman Preamp Master mix (ThermoFisher Scientific, Santa Clara, CA) per manufacturer's instructions. Quantitative PCR was performed to assess the expression of OLIG2, MYC, 18S rRNA and GAPDH SsoAdvanced Universal SYBR Green Supermix (Bio-Rad).

Gene expression analysis of OLIG2 and MYC was performed using the $2^{-\Delta\Delta C_t}$ method. For each cell, the number of CD63 positive EVs and the expression level of MYC and OLIG2 were calculated. In Fig 6, the 2D graphs were generated using GraphPad Prism Software version 5 (GraphPad, La Jolla, CA) and the 3D data were plotted using Matlab.

Acknowledgement

This work was performed in part at the San Diego Nanotechnology Infrastructure (SDNI) of UCSD, a member of the National Nanotechnology Coordinated Infrastructure, which is supported by the National Science Foundation (Grant ECCS-1542148). Research reported in this publication was partially supported by the National Institute of Biomedical Imaging and Bioengineering (NIBIB) of the National Institutes of Health under award number 1R43EB021129-01. The content is solely the responsibility of the authors and does not necessarily represent the official views of the National Institutes of Health.

Reference

1. Marusyk, A., Almendro, V. & Polyak, K., *Nat. Rev. Cancer*, 2012 **12**, 323.
2. Almendro, V., Marusyk, A. & Polyak, K., *Annu Rev Pathol*, 2013, **8**, 277–302.
3. Burrell, R. A., McGranahan, N., Bartek, J. & Swanton, C., *Nature*, 2013, **501**, 338.
4. Fidler, I. J., *Cancer Res*, 1978, **38**, 2651.
5. Polyak, K., *Nat. Methods*, 2010, **7**, 597, 599.
6. Dalerba, P., *Nat. Biotechnol.*, 2011, **29**, 1120.
7. Hunter, K., *Nat. Rev. Cancer*, 2006, **6**, 141.
8. Emmert-Buck, M. R., *Science*, 1996, **274**, 998.
9. Lee, K., *ACS Nano* aacs.nano, 2018, 7b07060
10. Mazutis, L., *Nat. Protoc*, 2013, **8**, 870.
11. Yu, Q., Heikal, A. A., *J. Photochem. Photobiol. B Biol*, 2009, **95**, 46.
12. Navin, N., *Nature*, 2011, **472**, 90.

13. Janes, K. a, Wang, C.-C., Holmberg, K. J., Cabral, K. & Brugge, J. S. , *Nat. Methods*, 2010, **7**, 311.
14. Tietjen, I. , *Neuron*, 2003, **38**, 161.
15. Gracz, A. D. , *Nat. Cell Biol*, 2015, **17**, 340.
16. Akers, J. C., Gonda, D., Kim, R., Carter, B. S. & Chen, C. C. , *J. Neurooncol*, 2013, **113**, 1.
17. Al-Nedawi, K. , *Nat. Cell Biol*, 2008, **10**, 619.
18. G Raposo, H W Nijman, W Stoorvogel, R Liejendekker, C V Harding, C J Melief, and H. J. G. B, *J. Exp. Med*, 1996, **183**, 1161.
19. Melo, S. A. , *Cancer Cell*, 2014, **26**, 707.
20. Shifrin, D. A., Beckler, M. D., Coffey, R. J. & Tyska, M. J. , *Mol. Biol. Cell* , 2013, **24**, 1253.
21. Kaern, M., Elston, T. C., Blake, W. J. & Collins, J. J. , *Nat. Rev. Genet*, 2005, **6**, 451.
22. Eldar, A. & Elowitz, M. B. , *Nature*, 2010, **467**, 167.
23. Im, H. , *Nat. Biotechnol*, 2014, **32**, 490.
24. Chevillet, J. R. , *Proc. Natl. Acad. Sci. U. S. A*, 2014, **111**, 14888.
25. Hoshino, A. , *Nature*, 2015, **527**, 329.
26. Akers, J. C. , *PLoS One* , 2016, **11**, e0149866.
27. Raj, A., van Oudenaarden., *Cell*, 2008, **135**, 216.
28. Chiu, Y.-J., Cai, W., Shih, Y.-R. V., Lian, I. & Lo, Y.-H. , *Small*, 2006, **12**, 3658.
29. Chiu, Y.-J., Cai, W., Lee, T., Kraimer, J. & Lo, Y.-H. , *BIO-PROTOCOL*, 2017, **7**.
30. Raposo, G. & Stoorvogel, W. , *J. Cell Biol*, 2013, **200**, 373.
31. Colombo, M., Raposo, G. & Théry, C. , *Annu. Rev. Cell Dev. Biol*, 2014, **30**, 255.
32. van der Pol, E., Böing, A. N., Harrison, P., Sturk, A. & Nieuwland, R. , *Pharmacol. Rev.* , 2012, **64**, 676.
33. Meacham, C. E. & Morrison, S. J. , *Nature*, 2013, **501**, 328.
34. Attayek, P. J., Hunsucker, S. A., Sims, C. E., Allbritton, N. L. & Armistead, P. M. , *Integr. Biol. (Camb)* , 2016, **8**, 1208.
35. Zhang, K. , *J. Am. Chem. Soc*, 2014, **136**, 10858.
36. Ungai-Salánki, R. , *Sci. Rep*, 2016, **6**, 1.
37. Kozono, D. , *Proc. Natl. Acad. Sci*, 2015, **112**, E4055.
38. Chan, JA. , *Cancer Res*, 2005, **65**, 6029.
39. Kowal, J., Tkach, M., Théry, C. , *Cell Biol.* , 2014, **29**, 116.
40. Logozzi, M. , *PLoS One*, 2009, **4**, e5219 .
41. Elmageed, Z. Y. A. , *Stem Cells*, 2014, **32**, 983.

42. Peinado, H. , *Nat. Med*, 2012, **18**, 883.
43. Li, Z., Wang, H., Eyler, C. E., Hjelmeland, A. B. & Rich, J. N. , *J. Biol. Chem*, 2009, **284**, 16705.
44. Ligon, K. L. , *Neuron*, 2007, **53**, 503.